

Electronic Supplementary Information

Hexagonal M_2C_3 ($M = \text{As}, \text{Sb}, \text{and Bi}$) Monolayers: New Functional Materials with Desirable Band Gap and Ultrahigh Carrier Mobility

Peng-Fei Liu,^{a,b,c,f} Tao Bo,^{b,c} Zhifeng Liu,^{a,e} Olle Eriksson,^h Fangwei Wang,^{c,g} Jijun Zhao,^{*a,d} and
Bao-Tian Wang,^{*b,c,f}

^aBeijing Computational Science Research Center, Beijing 100094, China

^bInstitute of High Energy Physics, Chinese Academy of Sciences (CAS), Beijing 100049, China

^cDongguan Neutron Science Center, Dongguan 523803, China

^dKey Laboratory of Materials Modication by Laser, Ion and Electron Beams (Dalian University of Technology), Ministry of Education, Dalian 116024, China

^eSchool of Physical Science and Technology, Inner Mongolia University, Hohhot 010021, China

^fCollaborative Innovation Center of Extreme Optics, Shanxi University, Taiyuan, Shanxi 030006, China

^gBeijing National Laboratory for Condensed Matter Physics, Institute of Physics, Chinese Academy of Sciences, Beijing 100080, China

^hDepartment of Physics and Astronomy, Division of Materials Theory, Uppsala University, Box 516, SE-75120 Uppsala, Sweden

E-mail: zhaojj@dlut.edu.cn; wangbt@ihep.ac.cn

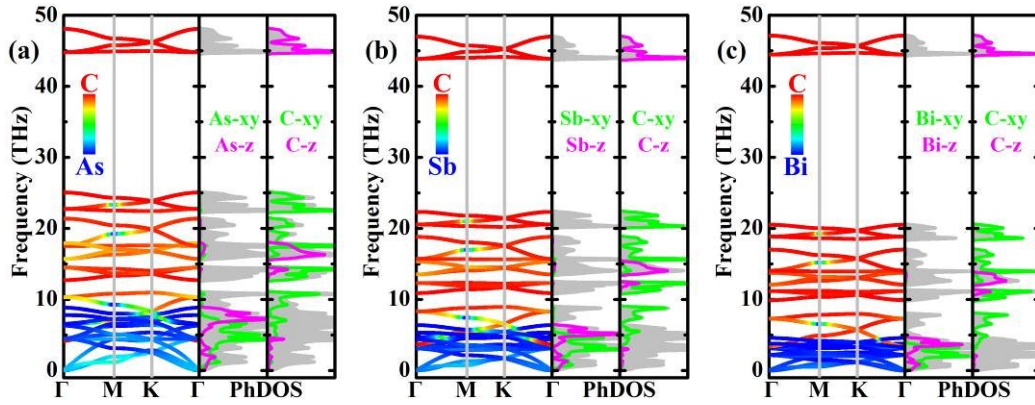


Figure S1. The orbital-resolved phonon spectra and projected phonon density of states for the M_2C_3 monolayers.

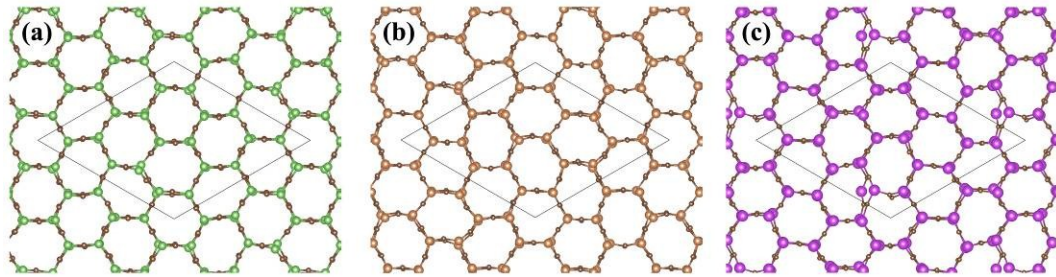


Figure S2. The top views of (a) As_2C_3 , (b) Sb_2C_3 , and (c) Bi_2C_3 monolayers after the ab-initio molecular dynamics simulation at 1000 K.

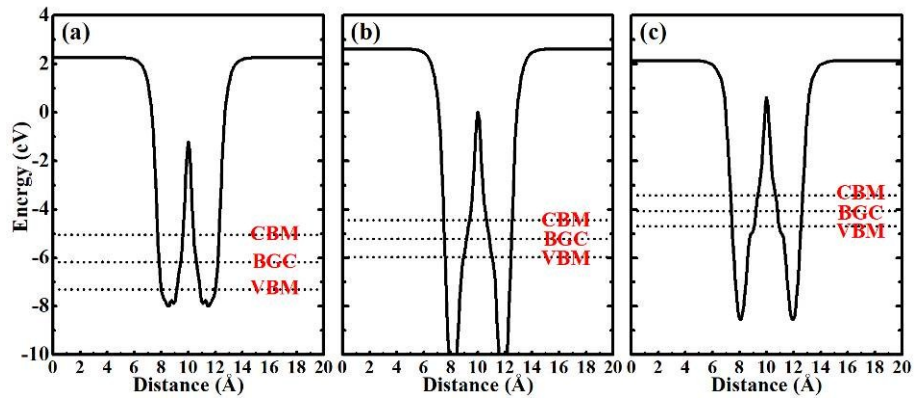


Figure S3. Average electrostatic potential (red curve) of (a) As_2C_3 , (b) Sb_2C_3 , and (c) Bi_2C_3 monolayers along the direction perpendicular to the layers calculated with the HSE06 functional. The conduction band minimum and valence band maximum (CBM and VBM) are shown, along with the bandgap center (BGC) energy.

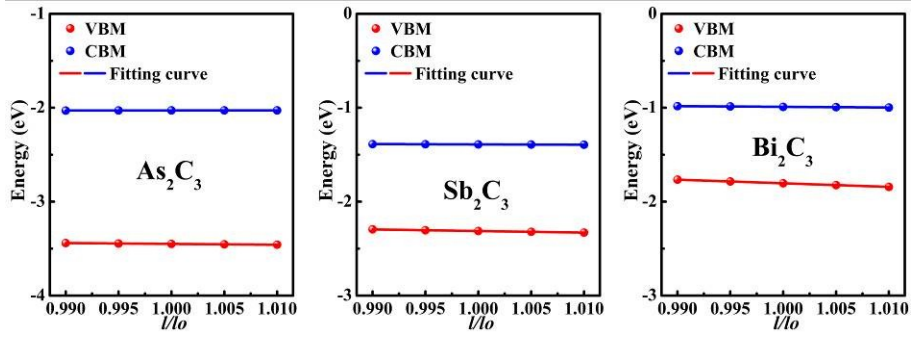


Figure S4. Band edge position shifts of the VBM (black dots) and CBM (red dots) subject to lattice distortion for the M_2C_3 monolayers.

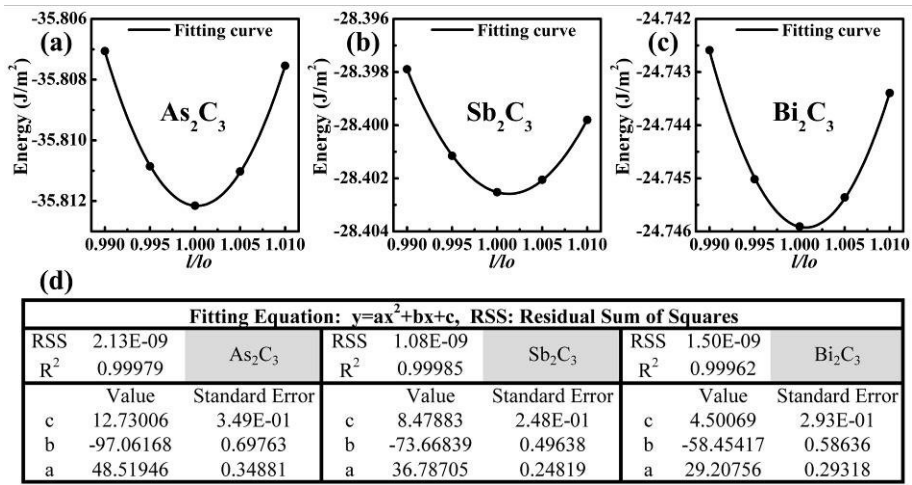


Figure S5. Total energy-strain curve of the M_2C_3 monolayers.

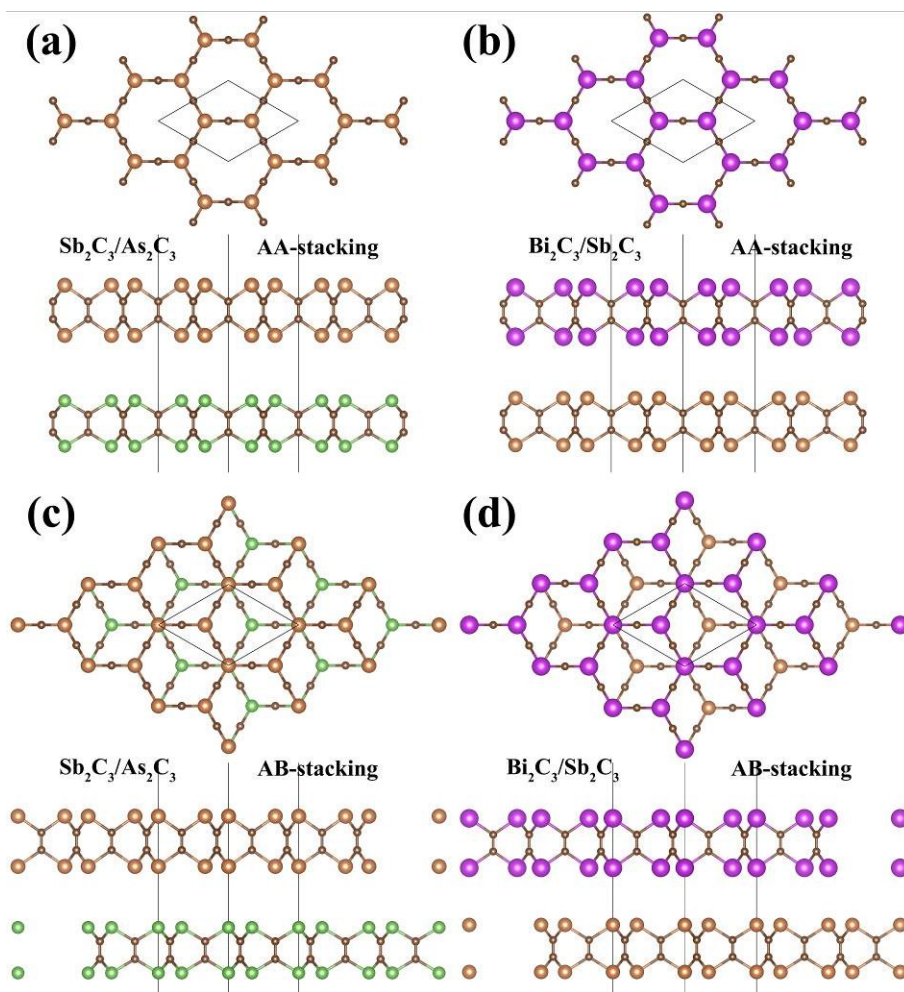


Figure S6. The possible stacking configurations of the bilayer are (a) AA-stacking $\text{Sb}_2\text{C}_3/\text{As}_2\text{C}_3$, (b) AA-stacking $\text{Bi}_2\text{C}_3/\text{Sb}_2\text{C}_3$, (c) AB-stacking $\text{Sb}_2\text{C}_3/\text{As}_2\text{C}_3$, and (d) AB-stacking $\text{Bi}_2\text{C}_3/\text{Sb}_2\text{C}_3$.

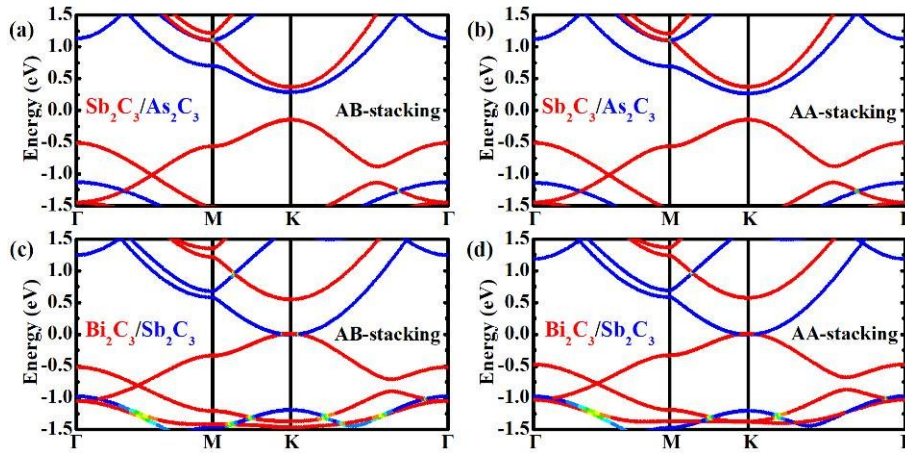


Figure S7. The resolved band structure of four heterojunctions. (a) AB-stacking $\text{Sb}_2\text{C}_3/\text{As}_2\text{C}_3$, (b) AA-stacking $\text{Sb}_2\text{C}_3/\text{As}_2\text{C}_3$, (c) AB-stacking $\text{Bi}_2\text{C}_3/\text{Sb}_2\text{C}_3$, and (d) AA-stacking $\text{Bi}_2\text{C}_3/\text{Sb}_2\text{C}_3$.

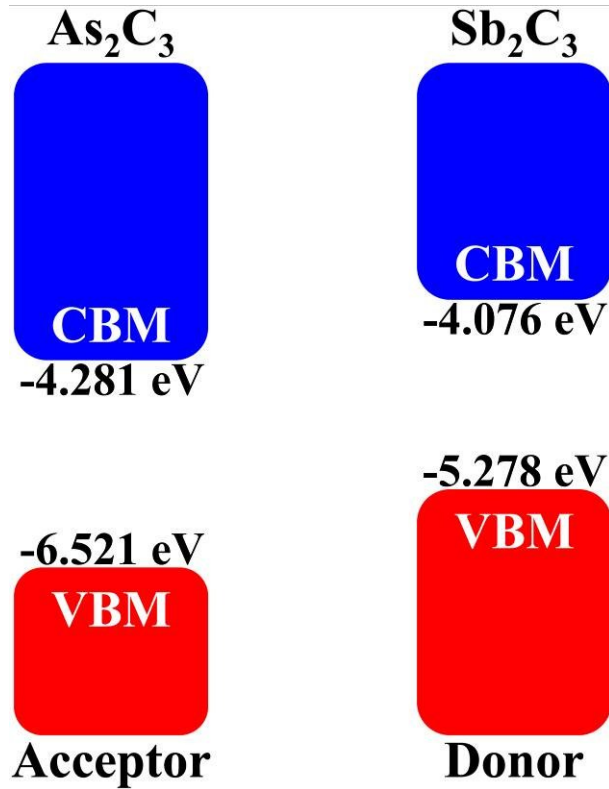


Figure S8. Band offsets between As_2C_3 and Sb_2C_3 monolayers for AB-stacking $\text{Sb}_2\text{C}_3/\text{As}_2\text{C}_3$ based on HSE06 method.

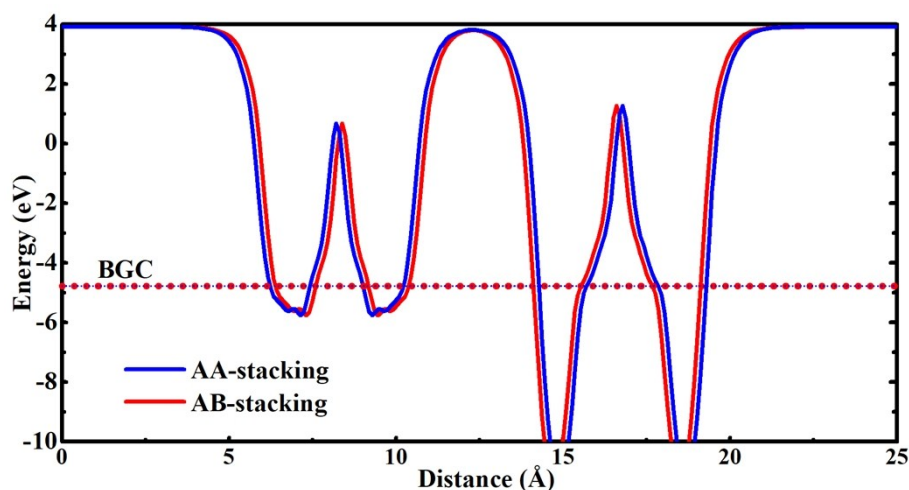


Figure S9. Average electrostatic potential of (blue curve) AA-stacking and (red curve) AB-stacking $\text{Sb}_2\text{C}_3/\text{As}_2\text{C}_3$, respectively, along the direction perpendicular to the layers calculated with the HSE06 functional. The bandgap center (BGC) energy is -4.779 and -4.772 eV for AA-stacking and AB-stacking $\text{Sb}_2\text{C}_3/\text{As}_2\text{C}_3$.

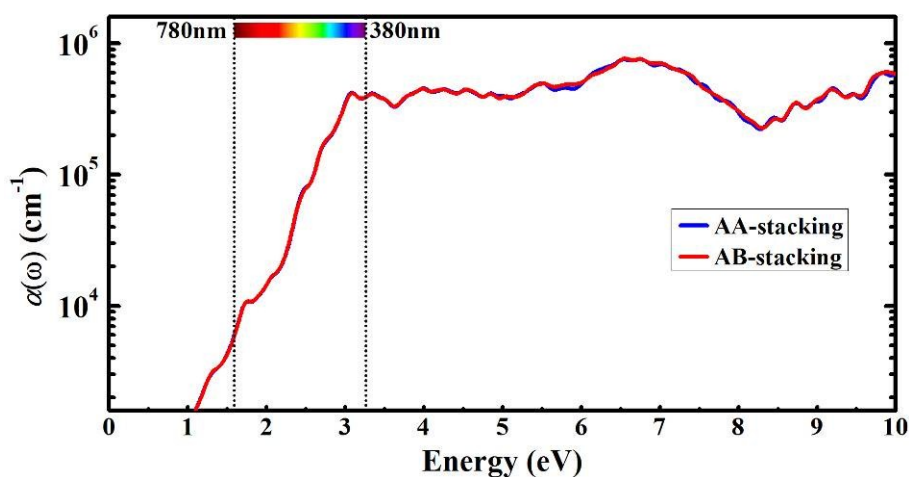


Figure S10. Optical absorption coefficients $\alpha(\omega)$ for (blue curve) AA-stacking and (red curve) AB-stacking $\text{Sb}_2\text{C}_3/\text{As}_2\text{C}_3$, respectively, based on HSE06 level. The seven-colour-light area between the dashed lines represents the visible light range (380 ~ 780 nm).

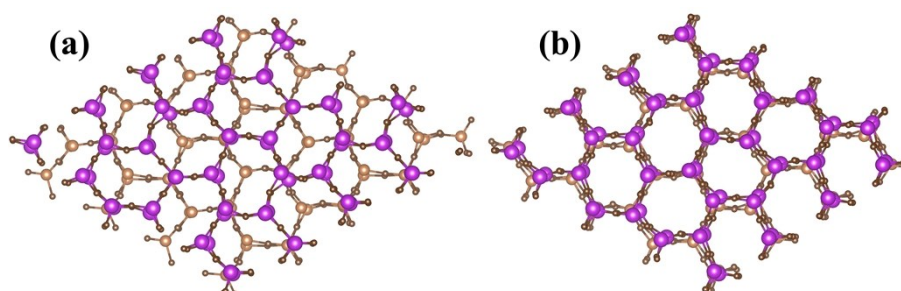


Figure S11. The top views of (a) AB-stacking $\text{Bi}_2\text{C}_3/\text{Sb}_2\text{C}_3$ and (b) AA-stacking $\text{Bi}_2\text{C}_3/\text{Sb}_2\text{C}_3$ after the ab-initio molecular dynamics simulation at 1000 K.

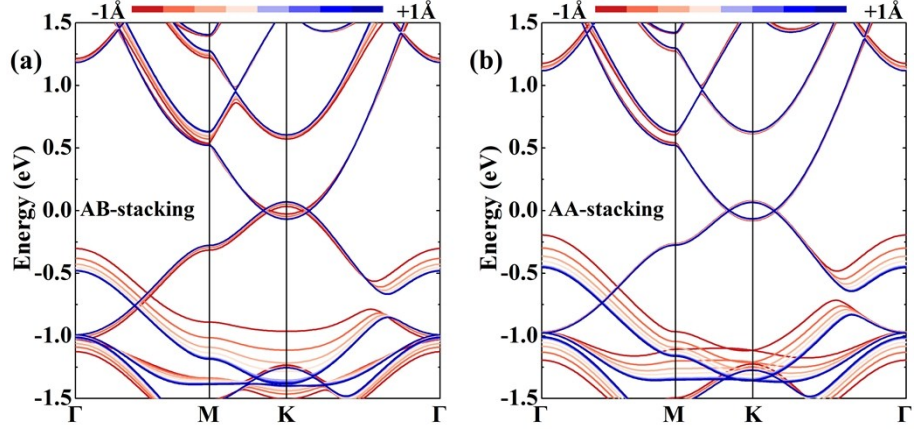


Figure S12. The band structures with the interlayer interaction distances increasing or decreasing 1 Å for (a) AB-stacking $\text{Bi}_2\text{C}_3/\text{Sb}_2\text{C}_3$, and (b) AA-stacking $\text{Bi}_2\text{C}_3/\text{Sb}_2\text{C}_3$.

Table S1. Calculated lattice constants (l_a), cohesive energies (E_{coh}), and band gaps for M_2C_3 sheets. The calculated cohesive energies demonstrate that the AB-stacking configuration is more stable than the AB-stacking one by ~ 0.89 and 8.79 meV for $\text{Sb}_2\text{C}_3/\text{As}_2\text{C}_3$ and $\text{Bi}_2\text{C}_3/\text{Sb}_2\text{C}_3$ heterojunctions.

Comp.	Patter	l_a (Å)	E_{coh} (eV)	HSE (eV)
$\text{Sb}_2\text{C}_3/\text{As}_2\text{C}_3$	AA	6.12	-4.98	0.96
	AB	6.12	-4.98	0.99
$\text{Bi}_2\text{C}_3/\text{Sb}_2\text{C}_3$	AA	6.54	-4.76	0
	AB	6.52	-4.76	0